

Article

Agricultural Residues of Lignocellulosic Materials in Cement Composites

Patrícia Ferreira Ponciano Ferraz ^{1,*}, Rafael Farinassi Mendes ², Diego Bedin Marin ¹,
Juliana Lobo Paes ³, Daiane Cecchin ⁴ and Matteo Barbari ⁵

¹ Department of Agricultural Engineering, Federal University of Lavras, Lavras 37200-000, Brazil; db.marin@hotmail.com

² Department of Engineering, Federal University of Lavras, Lavras 37200-000, Brazil; rafael.mendes@ufla.br

³ Department of Engineering, Campus Seropédica, Rural Federal University of Rio de Janeiro, Seropédica 23890-000, Brazil; julianapaes@ufrj.br

⁴ Department of Agricultural Engineering and Environment, Federal University of Fluminense, Niterói 24220-900, Brazil; daianececchin@id.uff.br

⁵ Department of Agriculture, Food, Environment and Forestry, University of Florence, Via San Bonaventura, 13-50145 Florence, Italy; matteo.barbari@unifi.it

* Correspondence: patricia.ponciano@ufla.br

Received: 28 October 2020; Accepted: 10 November 2020; Published: 12 November 2020



Abstract: Lignocellulosic material residues in cement composites are a favourable option for new fibre cement formulations in building materials, because they combine good mechanical properties with low density. This study aimed to evaluate the chemical, physical, anatomical, and mechanical properties of five cement panels reinforced with the following lignocellulosic materials: eucalyptus, sugarcane bagasse, coconut shell, coffee husk, and banana pseudostem. Lignocellulosic cement panels were produced with each lignocellulosic material residue, and three replicates of each type of lignocellulosic material were examined (15 panels in total). The lignin, extractives, ash, and holocellulose were examined. After 28 days of composite curing, the following physical properties of the panels were evaluated: density, porosity, water absorption after immersion for 2 and 24 h, and thickness swelling after immersion for 2 and 24 h. Mechanical tests (compression strength, internal bonding, modulus of rupture, and modulus of elasticity) were performed before and after the accelerated ageing test with a universal testing machine. Scanning electron microscopy and supervised image classification were performed to investigate the morphologies of the different materials and the filler/matrix interfaces. Eucalyptus and sugarcane panels had the best results in terms of the evaluated properties and thus, could potentially be used as non-structural walls. However, banana pseudostem, coconut shell, and coffee husk panels had the worst results and therefore, under these conditions, should not be used in building.

Keywords: lignocellulosic panels; chemical properties; physical-mechanical properties; residue materials

1. Introduction

The growing global population density has increased industrial development and intensified agricultural methods. The high productivity of agricultural species is the main cause of the large volume of agricultural residues generated [1]. Currently, these residues are either burnt or landfilled, thus resulting in several problems such as air pollution, emission of greenhouse gases, and occupation of useful land [2]. Given the worldwide population increase, housing problems are becoming a priority [3]. Thus, solutions to make sustainable houses more affordably are desirable. Many studies have focused on the use of natural materials in buildings, because these materials have high sustainability [4].

Therefore, the use of lignocellulosic material residue in cement composites is considered a good option for new fibre cement formulations to be used as building materials [5,6]. Natural fibres-reinforced composites combine acceptable mechanical properties with low density. Such composites have several well-known advantages, including low cost, use of available renewable natural resources, and biodegradability [7,8]. On the other hand, the use of natural fibres can be responsible for maintaining the mechanical properties in the long term. The inclusion of lignocellulosic materials for cement composite production is highly challenging because of the chemical properties of the lignocellulosic material, which may cause adverse effects during cement solidification.

According to [9], cement-bonded panels are manufactured from a mixture of Portland cement, chemical additives, and particles generated from lignocellulosic materials. Generally, these products combine the favourable qualities of cement (relatively high resistance to water, fire, fungus, and termite infestation) with those of lignocellulosic materials (high strength to weight ratio and workability) [9–11]. Producing cement composites by using agricultural lignocellulosic wastes, beyond allowing for waste reuse, enables the suitable properties of the material to be maintained; therefore, cement-lignocellulosic panels have been broadly applied in construction [10,12,13].

Studies aiming to produce cement composites reinforced with lignocellulosic materials for construction purposes have been intensified to make usage of these products technically and economically feasible [1,14]. Lignocellulosic fibres may potentially be used as reinforcement, because of their optimal mechanical performance, availability, and lower cost than that of the synthetic fibres usually applied in air-cured fibre-cement [15]. Therefore, the physical-mechanical properties and durability of cement-based composite properly reinforced with lignocellulosic materials are directly influenced by the type of vegetable matter used in the reinforcement; their chemical, physical, anatomical, and mechanical properties; and their production methods, among other variables [6].

The present work aimed to evaluate the effects of the chemical, anatomical, and physical compositions of different lignocellulosic materials on the physical and mechanical properties of cemented panels before and after accelerated ageing.

2. Materials and Methods

2.1. Lignocellulosic Materials

For production of the lignocellulosic residue cement composites, the following lignocellulosic materials were used: eucalyptus (*Eucalyptus grandis*), sugarcane bagasse (*Saccharum officinarum*), coconut shell (*Cocos nucifera*), coffee husk (*Coffea arabica*), and banana pseudostem (*Musa acuminata*).

Eucalyptus tree wood and banana pseudostem were obtained from local experimental cultivation at the Federal University of Lavras—UFLA. Sugarcane was obtained from a commercial cachaça distillery producing sugarcane liquor (cachaça) in Lavras, Minas Gerais state (MG), Brazil. The coconut shell was collected from local floriculture in Lavras, MG, Brazil. Coffee husk was obtained from a farm in the municipality of Santo Antônio do Amparo, MG, Brazil.

Eucalyptus wood was cut into short logs, which were passed through a laminator for delaminating. Coconut shell, sugarcane bagasse, coffee husk, banana pseudostem, and eucalyptus wood veneers were processed in a hammermill. The material particles were selected through sieving, and the fraction retained between 20 (0.841 mm) and 40 (0.420 mm) mesh sieves was used to produce the composites.

The particles of the lignocellulosic residues were treated with an alkaline solution to remove compounds that might hinder cement solidification. The alkaline treatment followed the procedures described in Ferraz [16] and Asgher [17], in which the particles were immersed in NaOH solution (5%) for 48 h.

2.2. Chemical, Physical, and Morphological Characterization of the Lignocellulosic Materials

The holocellulose content was calculated by extraction of lignin with sodium chlorite and acetic acid, according to the procedure reported in Browning [18]. The total extracted content was measured as established in the NBR 14853 Standards [19].

The insoluble lignin content was measured according to the NBR 7989 Standards [20]. An oven was used to obtain the mineral content of ash, according to the NBR 13999 Standards [21].

The morphological characterization of the lignocellulosic materials was performed in ImageJ® software. The length, diameter, and slimness index were obtained from 30 measurements for each type of lignocellulosic material. The slimness index was calculated by dividing the length by the diameter of each evaluated sample.

The density of lignocellulosic material was calculated with the NBR 11941 Standard [22] with some modifications in the volume measurement (water displacement after addition of already saturated, with a graduated beaker).

2.3. Lignocellulosic Cement Composite Production

For each composite, a different lignocellulosic material residue was used: eucalyptus, sugarcane bagasse, coconut shell, coffee husk, or banana pseudostem. For the calculations of the components of each panel (lignocellulosic material, High Early Strength (HES) cement, water, and CaCl_2 , as additive), the method suggested by Souza [23] was used to determine the equivalent masses of components.

The following parameters were applied: material and cement ratio, 1:2.75; water and cement ratio, 1:2.5; hydration water rate of 0.25; CaCl_2 additive, 4% (according to cement mass); percentage of loss, 6%. The calculations were performed for a nominal composite density of 1.2 g/cm^3 .

Three replicates for each lignocellulosic material were examined, for a total of 15 panels (five treatments and three replicates).

For production of each panel, all components were weighed and then mixed in a concrete mixer. The total mass of the components for the three panels equivalent to each treatment was mixed at the same time.

After mixing, the mass of each panel was separated, weighed, and randomly distributed in aluminium moulds of $480 \times 480 \times 150 \text{ mm}$. The moulding and stapling were performed in a cold room temperature ($25 \text{ }^\circ\text{C}$) for 24 h, and then, the panels were kept in an air-conditioned chamber at a temperature of $20 \pm 2 \text{ }^\circ\text{C}$ and $65 \pm 3\%$ relative humidity to ensure uniform drying for 28 days.

2.4. Physical Properties of the Composites

For each lignocellulosic material evaluated, three lignocellulosic panels were produced. For the physical properties, we prepared two samples for each panel with dimensions of $152 \times 152 \text{ mm}$ according to the American Society for Testing and Material—ASTM D1037 [24].

The following physical properties were evaluated: density (D), porosity (P), thickness (T), water absorption after immersion for 2 h (WA2 h) and 24 h (WA24 h), and thickness swelling after immersion for 2 h (TS2 h) and 24 h (TS24 h).

The determination of the density of the composites was performed before the WA and TS tests. The density was calculated by dividing the mass (measured in analytical balance) by the volume calculated (base area multiplied by height, measured with callipers). P was determined according to the procedures described in the American Society for Testing and Material—ASTM C 948 [25]. The methods to determine the WA and TS were as outlined in the American Society for Testing and Material—ASTM D1037 [24]. The average of D, P, WA, and TS and standard deviations were based on the values of three replicates.

2.5. Mechanical Properties of Composites

The mechanical properties of the composites were determined according to the Deutsches Institut für Normung (DIN 52362) [26] and American Society for Testing and Material (ASTM D1037) [24] in an AROTEC (São Paulo, Brazil) universal machine with a load cell of 20 MN and testing rate of 5 mm/min . The internal bonding (IB) (Equation (1)), compression strength (CS) (Equation (2)),

modulus of rupture (MOR) (Equation (3)), and modulus of elasticity (MOE) (Equation (4)) in static bending were evaluated.

$$IB = \frac{P_s}{b \times l} \quad (1)$$

$$CS = \frac{P_b}{b \times l} \quad (2)$$

$$MOR = \frac{3 \times P_b \times L}{2 \times b \times h^2} \quad (3)$$

$$MOE = \frac{P_{bp} \times L^3}{4 \times b \times h^3 \times \gamma_p} \quad (4)$$

where P_s —the rupture load (N); b —the width of the specimen (mm); l —the length of the specimen (mm); P_b —the maximum load (N); P_{bp} —the load at the proportional limit (N), γ_p —the deflection corresponding to P_{bp} (mm); h —the thickness of the specimen (mm); L —the span (mm).

For the internal bonding (IB) and compression strength (CS) tests, four samples per panel were used for each test. Six samples per panel were tested for the modulus of rupture (MOR) and modulus of elasticity (MOE) tests. Three samples per panel were tested after 28 days of curing, and three samples per panel were tested after accelerated ageing.

2.6. Accelerated Ageing

Accelerated ageing aims to speed up natural weathering in the laboratory by using soaking and drying cycles. This technique has been described by Almeida et al. [27]. In this process, the samples were successively immersed in water at 20 ± 5 °C for 170 min and, after a 10-min interval, heated to 60 ± 5 °C for 170 min in a ventilated oven. Another interval of 10 min at room temperature preceded the subsequent cycle, as recommended by the European Committee for Standardization—EN 494 [28]. A total of six accelerated ageing cycles were performed to better identify the composites' mechanical behaviour changes.

2.7. Statistical Analyses

Physical and mechanical properties were subjected to analysis of variance, and the Tukey test was applied for pairwise comparisons (95% confidence intervals) to evaluate the differences in lignocellulosic materials.

2.8. Electron Microscopy

Scanning electron microscopy (SEM) was used to investigate the morphology of the different types of materials and the fibre/matrix interface. The samples were mounted on aluminium stubs with the aid of a double-sided carbon strip, metallized in a gold evaporator (SCD 050—Baltec), and analysed under a LEO EVO 40 XVP microscope (Carl Zeiss AG, Milan, Italy) with an applied tension of 20 kV. The samples were evaluated before and after the accelerated ageing of the panels.

2.9. FreeViz

FreeViz is an intelligent multivariate visualization approach described by Demšara et al. [29,30]. It is an optimization method that finds the linear projection and associated scatterplot that best separate instances of different classes. In a single graph, the resulting FreeViz visualization can provide a global view of the classification problem being studied, reveal interesting relations between classes and features, uncover feature interactions, and provide information about intra-class similarities. The mathematical foundations of FreeViz, the optimization method, and its utility in various datasets have been described [29,30].

This algorithm optimizes a linear projection and displays the projected data in a scatterplot. The target projection is found through a gradient optimization approach and aims at separating the instances of different classes in class-labelled data [30].

2.10. Image Supervised Classification

Image classification was performed with QGIS 2.18.13 software [31] by using the Semi-Automatic Classification Plug-In developed by Luca Congedo [32]. The plug-in performs supervised type classifications, in which users provide representative pixel samples for each class to be mapped. In this study, for each lignocellulosic composite, three classes were defined (I—voids; II—lignocellulosic materials; and III—matrix) before and after the accelerated ageing process. Ten samples were collected for each class, for a total of 30 samples per image. After classification, the classes were quantified as a percentage for each image. The Minimum Distance algorithm was used for classification; this algorithm calculates the Euclidean distance (x, y) between the spectral signatures of the pixel image and training spectral signatures according to the following Equation (5) [32]:

$$d(x, y) = \sqrt{\sum_{i=1}^n (x_i - y_i)^2} \quad (5)$$

where x is the spectral signature vector of an image pixel, y is the spectral signature vector of a training area, and n is the number of image bands.

Therefore, the distance is calculated for every pixel in the image, assigning the class of the spectral signature that is closer, according to the following discriminant function (6) [32]:

$$x \in C_k \iff d(x, y_k) < d(x, y_j) \forall k \neq j \quad (6)$$

where C_k is the land cover class k ; y_k is the spectral signature of class k ; and y_j is the spectral signature of class j .

3. Results and Discussion

Figure 1 presents the FreeViz algorithm of the chemical composition of the lignocellulosic material residues and displays the projected data in a scatterplot. In this figure, the colours are associated with each lignocellulosic material evaluated, and the colour position indicates which chemical components have greater or lesser effects on the composition of the lignocellulosic material. On the basis of the mean chemical components, the aptitude of the material is determined.

Table 1 presents the chemical composition statistical analyses of the different types of lignocellulosic material evaluated. The plant-based natural fibres consist of cellulose, hemicellulose, lignin, extractives, and ash, and their concentrations depend on factors such as fibre type, growth condition, dimension, age, location on the plant, and extraction and processing methods [33].

Figure 1 and Table 1 show the most influential chemical composition in each evaluated lignocellulosic material.

Banana pseudostem had the highest average content of ash among the lignocellulosic materials, and a lower content of lignin was evaluated. Coconut shell had the highest composition of lignin, but the lowest content of extractives and holocellulose. Eucalyptus showed an intermediate amount of lignin and holocellulose. Sugarcane had the highest extractives and the lowest ash values. In general, the results were consistent with those observed in other studies performing chemical analyses of different types of lignocellulosic materials [6,9,34].

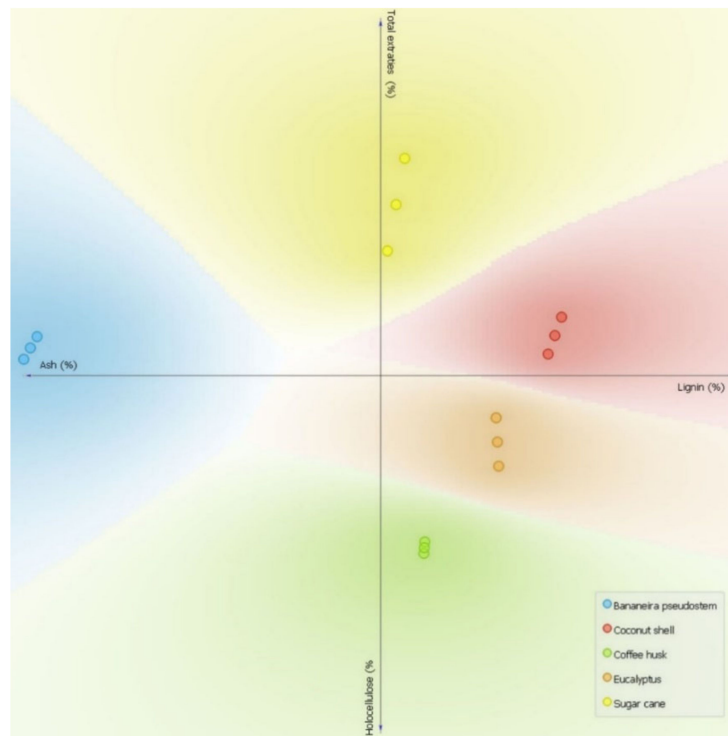


Figure 1. FreeViz optimization of the chemical composition of the lignocellulosic material residues.

Table 1. Averages and standard deviations of the chemical compositions of the lignocellulosic material residues.

Lignocellulosic Materials	Lignin (%)	Total Extractives (%)	Ash (%)	Holocellulose (%)
Eucalyptus	28.00 d (0.667)	11.65 b (0.145)	1.46 b (0.286)	58.90 b (1.098)
Sugar cane	17.34 b (0.667)	24.20 d (0.920)	0.84 a (0.037)	57.63 b (1.550)
Banana pseudostem	11.79 a (0.104)	17.97 c (0.350)	10.68 d (0.179)	59.55 b (0.275)
Coconut shell	39.07 e (0.041)	7.39 a (0.590)	3.65 c (0.204)	49.89 a (0.428)
Coffee husk	21.40 c (0.190)	12.35 b (0.025)	1.41 b (0.054)	64.87 c (0.269)
<i>p</i> value	0.0000	0.000	0.000	0.000
CV (%)	1.84	3.52	4.95	1.53

Averages followed by the same letter in the column are statistically equivalent according to the Tukey test at 5% significance. The values in parentheses are standard deviations. CV: coefficient of variation.

In most cases, the extractives are primarily responsible for the inhibition of cement solidification [1]. The extractives are resins and other chemicals that may migrate to the surface of the particle during the drying process, thus potentially resulting in the formation of a hydrophobic layer, which reduces the hydrogen bonds between the lignocellulosic material and cement, and consequently, increases the bonding strength [35].

The chemical composition of plant-based fibres strongly influences their mechanical properties because cellulose, hemicellulose, and lignin are primarily responsible for the bond behaviour and degradation of natural fibres in composites [33]. Coconut shell exhibited the highest lignin content,

whereas holocellulose exhibited the lowest lignin content. The lignin content in banana pseudostem was significantly lower than that in the other materials evaluated.

The total extractives content of the lignocellulosic materials evaluated showed significant differences. The extractive content is the most limiting factor in the production of cement composites because extractive action may result in lower resistance of the composites [36]. According to Fan et al. [11], extractives hinder cement curing and the interactions between lignocellulosic particles and the cement matrix, thus leading to empty spaces between the matrix and the lignocellulosic particles/fibres. Coconut shell had high levels of extractives (39.07%). In that case, the extractives may act as a barrier to satisfactory linkage between the particles and cement, but may be necessary to allow the treatment to achieve better composite properties [1]. Ash in lignocellulosic materials is the material remaining after incineration has removed the organic constituents [37]. Thus, the ash fraction comprises most of the inorganic substances present in the native substrate [38]. A higher amount of ash was observed in banana pseudostem, owing to its high mineral content. The same result has been found by Habibi et al. [8].

According to Teixeira et al. [6], holocellulose has a significant influence on the composite properties through the concentration of hemicellulose dissolved due to the higher alkalinity of the cement's hydration water. Hemicellulose can diminish the composite's resistance because it is one of the elements responsible for adherence between fibrils of the plant material and the arrangement of fibrils within the cement matrix.

Table 1 shows large differences among the chemical compositions of the lignocellulosic material residues evaluated. The variation in the proportions of the chemical constituents is influenced by the plant species; agricultural variables, such as soil quality, weathering conditions, the level of plant maturity, and the quality of the retting process; and measurement conditions that may include or exclude moisture [39]. Consequently, these factors may affect the physical and mechanical properties of the panels produced from those materials.

Table 2 shows the values obtained for the length, diameter, and slinness index of the lignocellulosic materials used as reinforcement for cement-based panels. Banana fibres had the highest length and diameter values. However, the highest slinness index and intermediate lengths were observed for coconut fibres. Coconut had the smallest diameter. Eucalyptus, sugarcane bagasse, and coffee husk showed the closest geometric characteristics, achieving the lowest values of length and intermediate diameters.

Table 2. Averages and standard deviations of the geometry and density properties of the lignocellulosic composites.

Lignocellulosic Materials	Length (cm)	Diameter (cm)	Slinness Index	Density (g/cm ³)
Eucalyptus	0.27 c (0.07)	0.07 b (0.01)	3.81 bc (0.96)	0.341 a (0.092)
Sugar cane	0.29 c (0.06)	0.05 c (0.01)	6.10 bc (1.54)	0.094 d (0.005)
Banana pseudostem	1.25 a (0.12)	0.18 a (0.03)	7.41 b (1.40)	0.237 b (0.008)
Coconut shell	0.64 b (0.17)	0.03 d (0.01)	21.93 a (9.46)	0.138 c (0.087)
Coffee husk	0.19 c (0.03)	0.08 b (0.02)	2.50 c (0.69)	0.167 c (0.007)
<i>p</i> value	0.0000	0.0000	0.0000	0.0024
CV (%)	25.09	26.29	61.74	6.31

Averages followed by the same letter in the column present statistical equality by the Tukey test at a 5% significance. The values in parentheses are the standard deviation. CV: coefficient of variation.

The geometric characteristics of the lignocellulosic materials directly influence the fibre/matrix interface. These characteristics allow for adequate covering and can increase the mechanical resistance of the produced panel; alternatively, they can generate a loss of interaction, which can increase the

number of pores, owing to curving or even folding inside the cement matrix, thus directly affecting the physical and mechanical properties of the composites produced [6,9].

The density values of the different types of lignocellulosic materials are shown in Table 2. There was a higher density for eucalyptus fibres (0.341 g/cm³) and a lower density for cane fibres (0.094 g/cm³).

Table 3 shows the physical properties of the composites produced with the lignocellulosic materials. The values obtained for the density of the composites in this study were between 0.984 (banana pseudostem) and 1.267 g/cm³ (coffee husk). The Bison Wood-Cement Board [40] determines the density of cement-based panels in the range of 1.250 g/cm³, when the panels are produced with wood particles. The density of the panel is dependent on the compaction of the material, pressing pressure, particle size, and the density of the raw material and the binding agent [41]. The variability in density was dependent on the combination of raw materials and their compaction, owing to the presence of particle–particle bonding, because the pressure and the cement ratio were constant for all panels [42]. Density is an important property because it correlates with many properties of the composite material, such as thermal and mechanical characteristics.

Table 3. Average and standard deviation of the physical properties of the lignocellulosic composites.

	Density g/cm ³	Porosity (%)	Water Absorption 2 h (%)	Water Absorption 24 h (%)	Thickness Swelling 2 h (%)	Thickness Swelling 24 h (%)
Eucalyptus	1.18 bc (0.068)	74.2 bc (2.073)	15.700 bc (0.991)	16.467 ab (0.977)	2.267 b (0.246)	6.467 b (0.435)
Sugar cane	1.17 abc (0.082)	78.5 bc (8.521)	5.200 a (0.678)	10.800 a (1.355)	1.067 a (0.789)	5.300 b (0.905)
Banana pseudostem	1.00 ab (0.022)	87.5 c (2.110)	26.034 d (0.805)	27.834 c (0.228)	1.834 ab (0.228)	2.867 a (0.146)
Coconut shell	0.98 a (0.082)	62.8 ab (5.100)	21.867 cd (5.410)	23.567 bc (5.339)	1.900 ab (0.365)	3.367 a (0.688)
Coffee husk	1.27 c (0.079)	52.5 a (9.702)	12.567 ab (3.024)	13.400 a (2.027)	1.267 ab (0.117)	2.134 a (0.360)
<i>p</i> value	0.0024	0.000	0.000	0.0001	0.034	0.000
CV (%)	6.31	8.92	17.46	14.44	25.50	13.71

Averages followed by the same letter in the column present statistical equality by the Tukey test at a 5% significance. The values in parentheses are the standard deviation. CV: coefficient of variation.

A relationship between density and porosity is observed in composites: the higher the density, the lower the porosity. Porosity results from the formation of air-filled cavities inside an otherwise continuous material, and it is often unavoidable in composites. Porosity develops during the mixing and consolidation of two different material parts: plant fibre composites typically contain a relatively high porosity, which may influence the properties and performance of the composites [43].

The panels produced with banana pseudostem had the lowest values of density and the highest values of porosity—findings associated with fibres with longer lengths and higher slimmness index values. Coffee husk panels had the lowest porosity values, the lowest slimmness index, and the highest density among the panels. Therefore, fibres with longer lengths are less able to interact with the matrix, thus causing more empty spaces in the composite, because of the difficulties in coverage and mixture with cement and fibre/matrix interactions.

However, these values are also influenced by the chemical composition of the material (Table 1). Higher amounts of holocellulose and intermediate values of extracts, such as coffee husk, influence the connection with the matrix and the curing of the cement, thus resulting in panels with higher densities and lower porosity values. Coconut shell panels, despite having the lowest extract values, had the lowest density among the panels, possibly because of the lower amount of holocellulose and the geometry of the reinforcement material. Similar findings were observed for sugarcane bagasse. Although sugarcane had the highest amount of extract, which affects the curing of panels [6,11], owing to the association with the geometry of the fibres, these panels showed the highest density

values. Thus, although the literature has described pronounced effects of extractives on cement curing, for cement-based panels, there is a composite effect of the material's geometry and chemical composition on the density and porosity, thus significantly influencing the other physical and mechanical properties of the obtained cement-based composites.

Table 3 shows the amount of water absorbed and the variation in the thickness during the first 2 h of immersion in water and between the first 2 and 24 h. Interestingly, the most significant absorption of water occurred during the first 2 h. After this period, the amount of water absorption was almost irrelevant for most materials, except for sugarcane (5.6%).

In contrast, after the 2 h of contact with water, the cumulative thickness swelling was much greater than that in the first 2 h, except for coffee husk (0.8%). According to these results, the process of water absorption is faster than the thickness swelling. The increase in thickness after 2 h was probably associated with the large amount of water absorbed during the first 2 h. In this case, in a building using these lignocellulosic composites, the first 2 h of contact with water would be critical for the panel's water absorption and thickness, owing to the effects on the mechanical properties of the composites. Such water absorption by the particles must be avoided for good dimensional stability. The greater the dimensional variation, the lower the binding with the matrix; therefore, limiting water absorption is thus often desirable [44].

Lignocellulosic materials can absorb substantial amounts of water. Banana pseudostem panels absorbed 26.034% of their weight in water. According to Mendes et al. [9], a lower content of lignin results in higher hydrophilicity. Banana pseudostem had the least amount of lignin (Table 1) and the lowest density values, thus resulting in the highest WA values (Table 3). A direct effect of panel density on the properties WA2 h and WA24 h was also observed, in which the panels with the highest densities (eucalyptus, sugarcane bagasse, and coffee husk) showed the lowest water absorption values.

The sugarcane panels notably showed low values of water absorption, which may be associated with the higher quantity of extracts in the sugarcane bagasse. Although the amount of extractives affects cement curing, when extractives are associated with the material, they can make the panels less hygroscopic [6,11], particularly in the first hours of contact with water. However, although the sugarcane panels presented the lowest TS2 h, sugarcane and eucalyptus panels had the highest TS24 h values. This finding may be explained by the dimensional expansion of the materials (sugarcane and eucalyptus), which had lower density than the other materials (Table 2), thus promoting greater dimensional movement of the panels and consequently, their expansion in thickness.

Although differences were observed among the panels with coffee husk, coconut shell, and 406 banana pseudostem, an evaluation of the density and porosity of these panels indicated that this effect was not reflected in the swelling in thickness (TS2 h and TS24 h). TS is more strongly influenced by the density of the lignocellulosic materials used to produce the panels.

Thickness swelling is a critical parameter in the dimensional stability of composites. The composite thickness can also vary according to the moisture content, particularly during contact with water. The characteristics of composites with lignocellulosic materials immersed in water are influenced by the nature of the fibre and matrix materials, the relative humidity, and the manufacturing technique, which determines factors such as the porosity and volume fraction of fibres [45].

In a similar study, Teixeira et al. [6] have evaluated fibre cement panels and found values of water absorption of 20.6, 17.4, 16.9, and 17.2 for eucalyptus, coffee husk, banana pseudostem, and coconut shell composite panels, respectively, after 7 days. Nasser et al. [46] have found values close to 4.73% for TS in evaluating cement composites with a density of 1.200 g/cm³. The Bison Wood-Cement Board [40] has established values of 0.8% for TS2 h and values between 1.2% and 1.8% for TS24 h. On the basis of Table 3, the proposed panels are not recommended for use in conditions involving contact with water, which could damage their structure. However, they are suitable for dry applications such as indoor rooms.

Beyond the physical properties, the mechanical building properties must be assessed to ensure adequate safety [47]. In this study, we evaluated the mechanical properties of the lignocellulosic panels before and after the accelerated ageing process in the laboratory (Table 4).

Table 4. Compression strength (CS), internal bonding (IB), modulus of rupture (MOR), and modulus of elasticity (MOE) of the lignocellulosic composites before and after the accelerated ageing process.

	Before Accelerated Ageing				After Accelerated Ageing	
	CS (MPa)	IB (MPa)	MOR (MPa)	MOE (MPa)	MOR (MPa)	MOE (MPa)
Eucalyptus	9.33 b (1.24)	0.54 c (0.06)	6.43 bA (0.25)	1462 a α (353)	5.60 bA (0.96)	1090 b α (111)
Sugar cane	2.81 a (0.80)	0.32 bc (0.15)	12.29 cA (0.25)	2070 a α (371)	5.56 bB (1.60)	970 b β (159)
Banana pseudostem	0.98 a (0.23)	0.07 a (0.01)	1.60 aA (0.87)	1528 a α (345)	1.16 aA (0.36)	117 a β (41)
Coconut shell	1.55 a (0.06)	0.30 abc (0.11)	3.47 aA (0.93)	3105 a α (646)	1.77 aA (0.94)	182 a β (101)
Coffee husk	2.23 a (0.69)	0.23 ab (0.05)	3.78 abA (1.88)	1572 a α (469)	0.28 aA (0.16)	53 a β (9)
<i>p</i> value	0.000	0.0011	0.000	0.3155	0.0001	0.0000
CV (%)	21.79	30.87	18.58	49.51	33.08	20.60

Averages followed by the same letter (lowercase for lignocellulosic materials in the columns, uppercase for MOR before or after accelerated ageing tests in the lines, and Greek letters for MOE) presented statistical equivalence according to the Tukey test at 5% significance. The values in parentheses are standard deviations. CV: coefficient of variation.

The results in Table 4 show that the lignocellulosic material affected the mechanical properties of composites. The eucalyptus composites had the best results in CS and IB. Eucalyptus wood panels had significantly higher average values of CS, whereas the other types of panels were lower and statistically equivalent. This finding may be explained by the resistance characteristics of each material. Eucalyptus presents resistance in the compression test [48], and the material has high density (Table 2), which allows for a lower volume of lignocellulosic material in the matrix and consequently, fewer defects due to the fibre/matrix interaction. For the IB, the panels with eucalyptus, sugarcane bagasse, and coconut shell were statistically equivalent and had the highest average values. The lowest value of IB was obtained for panels with banana pseudostem, owing to the greater lengths of the fibres used (Table 2), higher porosity values (Table 3), and the low fibre-to-fibre interaction matrix. The coffee husk panels, despite having the highest density and lowest porosity values, did not present a good fibre/matrix interaction and thus, did not have good internal bonding properties. Sugarcane bagasse panels had the lowest density among the evaluated materials, thus resulting in a greater surface area for covering by cement. Owing to their adequate geometric relationship, sugarcane bagasse panels had an adequate fibre–cement interaction.

In general, the lowest values of CS and IB were associated with the low adhesion of matrix fibre in the composite, thus making the panels weak, allowing for easy decoupling of fibres, and favouring crack propagation and fragility of the composite [49,50]. Moreover, the fibre matrix interaction in cement-based panels was more affected by the geometric and chemical characteristics than by the physical properties of lignocellulosic materials.

The statistical analysis indicated different significance ($p < 0.05$) values for the mechanical properties before and after the accelerated ageing process in the laboratory.

Sugarcane bagasse panels showed the highest mean MOR values, differing statistically from the other types of panels. Eucalyptus panels showed the second-best performance in terms of this

property. However, after accelerated ageing, no statistical difference was observed between the cane bagasse and eucalyptus panels for MOR. Sugarcane bagasse panels were the only panels showing a significant reduction in resistance values after accelerated ageing. This result was a consequence of the dimensional movement of the panels due to the greater volume of sugarcane bagasse particles present, because the lower density of the material (Table 2) promoted swelling of the panel (Table 3) and separation of the particles and matrix, and consequently, an increase in empty spaces.

The MOE before ageing showed no statistical difference between treatments. However, significant reductions in the values of MOE were observed after the accelerated ageing of the cane bagasse, coconut shell, and coffee shell panels. After accelerated ageing, eucalyptus and sugarcane bagasse showed the highest average MOE values, a notable result suggesting that it is the most appropriate material, in terms of mechanical properties, for the production of cement-based panels.

The values of the mechanical properties of cement-based panels decreased as a result of exposure of the samples to varying water content under extreme temperature conditions. Prolonged soaking in water may decrease the fibre–matrix interface and fibre resistance, owing to the alkaline degradation of lignocellulosic materials [51,52], and increase the porosity of composites [46,53]. Furthermore, based on the analysis of MOR and MOE tests carried out before and after the accelerated ageing process (Table 4), it is possible to evaluate the durability of the composites. The test showed a decrease in strength and stiffness of 12 to 92% and 25 to 96%, respectively, dependent on the lignocellulosic material. Based on these results, panels with Eucalyptus obtained the greatest durability and panels with coffee husk presented the worst durability.

The Bison Wood-Cement Board [40] has determined a minimum value of 9 MPa for MOR and 3000 MPa for MOE. Thus, only the sugarcane bagasse panels met the MOR criteria, and only the coconut shell panels met the MOE criteria, even before the accelerated ageing process. These findings are due to the low density of these lignocellulosic materials that resulted in a weak fibre–matrix interface, thus causing lower mechanical resistance. Nevertheless, these panels could still be used as sealing systems without structural load. To use these structurally loaded panels, new production variables must be evaluated, such as lower percentages of reinforcement material depending on the proportional density and the geometric and chemical characteristics.

In Figures 2 and 3, to investigate the surface morphology of the fillers, we collected SEM images of the fracture surface before and after the ageing accelerated process. Image supervised classification (ISC) was performed to classify the percentages of the three studied classes: I—voids; II—lignocellulosic materials; and III—matrix of the same images.

Figures 2 and 3 show the SEM analysis of the fibre–matrix interface of the composites. Regardless of the lignocellulosic material type, the fracture surfaces of the composites showed large cracks and boundaries between the lignocellulosic material and the matrix. Moreover, numerous fibre pull-outs and voids were observed on the surfaces, thus indicating the poor interfacial adhesion between the components.

Because of the elongated nature of strands, some difficulties are expected in mixing the lignocellulosic materials with cement, thus potentially leading to incomplete coating/wetting of the particles with cement [9] and void formation. The presence of voids is considered the most critical defect affecting a composite's mechanical properties [54]. Voids prevent the load from being effectively transferred to the particles from the matrix, thus leading to debonding of the particles of lignocellulosic materials and to low mechanical properties of the composites. The physical-mechanical properties of cementitious composites are directly associated with the adhesion of fibres with the matrix [14]. The lower MOR and MOE values (Table 3) observed may be associated with the loss of adhesion of the fibres with the matrix (Figures 2 and 3). Thus, the SEM results were consistent with the mechanical results.

The surface of sugarcane composite was smoother than the surfaces of the other lignocellulosic composites. Figure 2 and Table 3 show that sugarcane and eucalyptus had higher adhesion with the matrix. In these composites, the fracture surface showed a highly homogenous texture, suggesting

good dispersion and compatibility, although some voids and protruding lignocellulosic particles were observed in the fracture surfaces. The presence of voids caused by the movement of the fibres of the lignocellulosic materials resulted in an increased water absorption capacity.

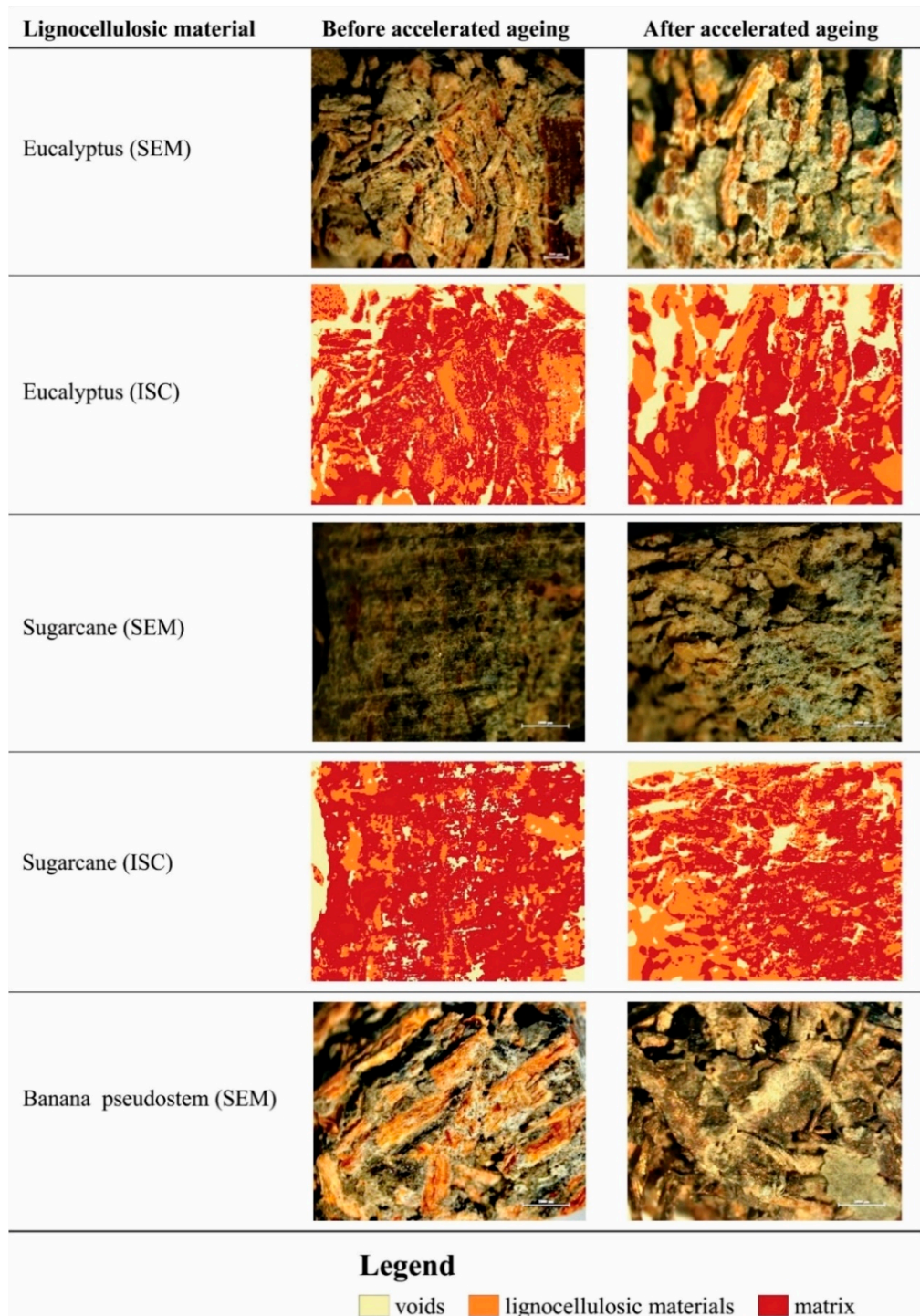


Figure 2. Scanning electron microscopy (SEM) images and image supervised classification (ISC) of the evaluated lignocellulosic materials before and after the accelerated ageing process.

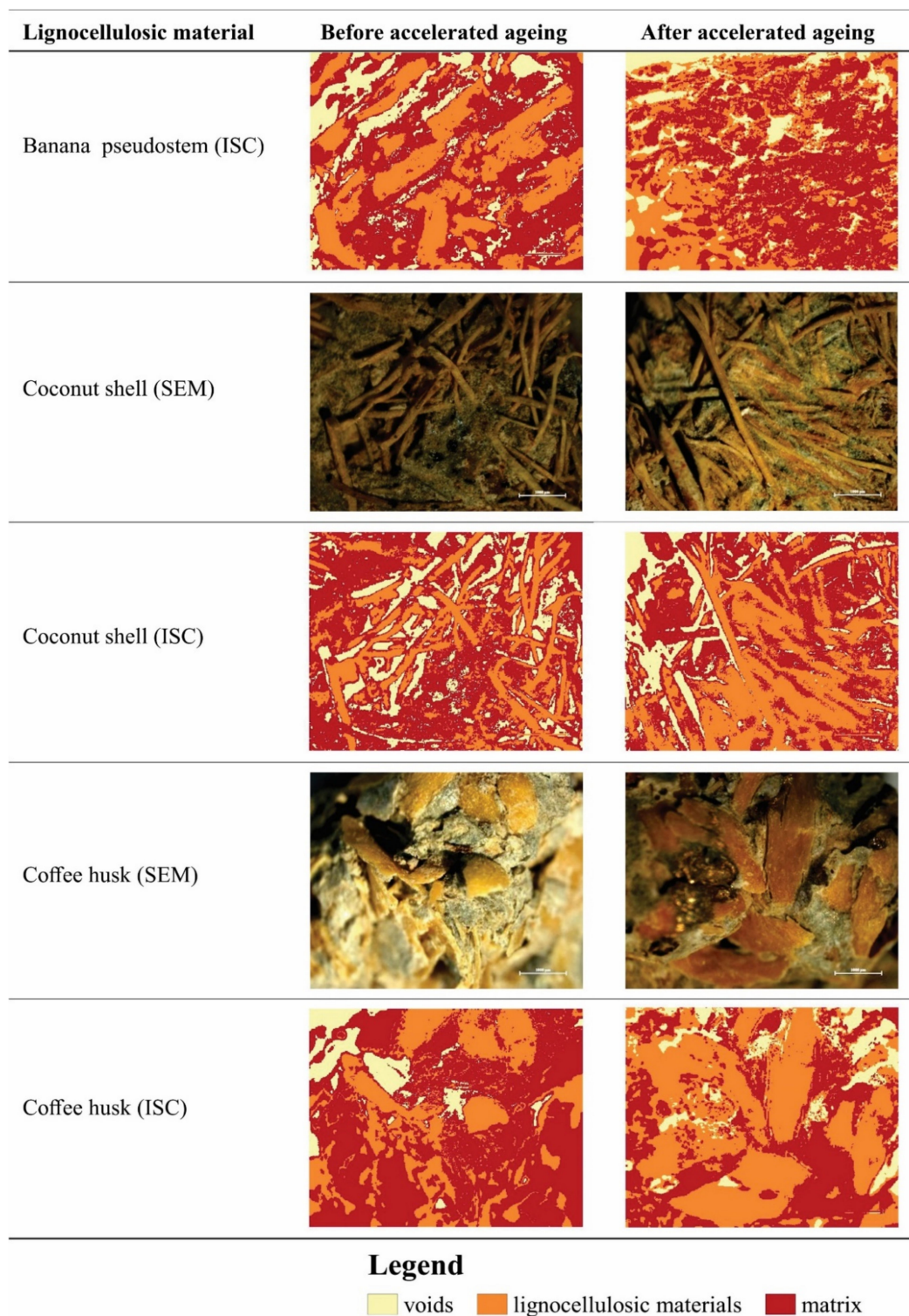


Figure 3. Scanning electron microscopy (SEM) images and image supervised classification (ISC) of the evaluated lignocellulosic materials before and after the accelerated ageing process.

Figures 2 and 3 show the consequences of the accelerated ageing process on the microstructures of the composites. Degradation of the fibres was observed after the accelerated ageing tests. According to Lepage [55], the principal factors that promote material degradation under weathering are moisture, sunlight, and heat. The accelerated ageing test evaluated two of these factors (moisture and heat) [56]. The adhesion of the lignocellulosic material in the fibre–matrix interface exposed to the accelerated

ageing process was lower than that before the exposure. We observed damage at the interface as a result of the accelerated ageing process, thus causing variations in the volume of the fibres. Similar results have been found by Fonseca et al. [14]. In addition, according to Fiorelli et al. [56], this degradation of the fibres and variation in the volume may directly influence the performance of the composites, because the fibres are responsible for supporting the mechanical load imposed on the composite material.

The nearest neighbour supervised rating clearly defined the distribution of the lignocellulosic materials, matrix, and voids. According to the number of pixels, we calculated the percentage of lignocellulosic materials, matrix, and void for each lignocellulosic composite before and after the accelerated ageing process (Figure 4).

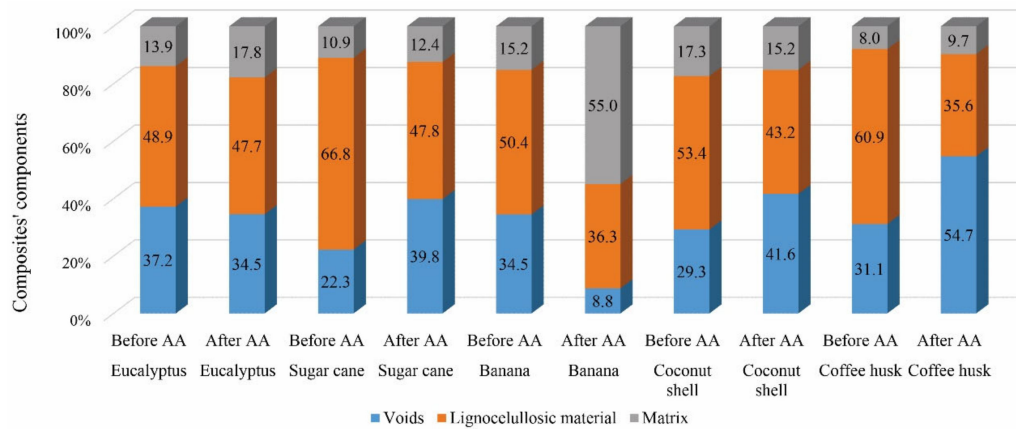


Figure 4. Composite components obtained through supervised image analysis of the evaluated lignocellulosic material before and after the accelerated ageing (AA) process.

Figure 4 shows the differences in the amounts of lignocellulosic materials, matrix, and void before and after the accelerated ageing test. After the accelerated ageing test, a proportional decrease was observed in the percentage of lignocellulosic material, and an increase was observed in the amount of matrix. It is possible to observe that after the aging test, as the lignocellulosic particle volume decreases (Figure 4), the resistance to the applied stress decreases too, thereby decreasing panel strength. This reduction in the mechanical properties after the accelerated ageing test of the composites is shown in Table 4. The mechanical properties of the composite materials were proportional to the fibre volume fraction: the greater the amount of fibres, the higher the mechanical properties. Table 5 provides the correlation values of the amount of lignocellulosic materials and the mechanical properties before and after the ageing process. Based on these results, it is possible to observe the high and positive values, which means that if the amount of lignocellulosic material increases, it also increases the values of MOE and MOR before ageing and after ageing. However, there is a limit to the amount of fibres above which the mechanical properties of composites begin to deteriorate, mainly because the quantity of cement is insufficient to properly wet all the fibres, thus resulting in weak fibre/matrix interfacial adhesion and increased porosity, and hence, poor mechanical properties [54].

Table 5. Correlation values of the amount of lignocellulosic material in the panel and modulus of rupture (MOR) and modulus of elasticity (MOE) of the lignocellulosic composites before and after the accelerated ageing (AA) process.

	Amount of Lignocellulosic Material in the Panel	
	Before AA	After AA
MOR before AA	0.678	-
MOE before AA	0.108	-
MOR after AA	-	0.936
MOE after AA	-	0.900

4. Conclusions

The results of this study improve understanding of the effects of the chemical, physical, and anatomical properties of lignocellulosic materials on the physical and mechanical properties of cement-based panels.

Although the literature has suggested that chemical composition has the most pronounced effect on the quality of cement-based products, we observed associated effects of the material's geometry and chemical composition, which directly affected the fibre–matrix interaction and consequently, the physical and mechanical properties of the panels.

The density of lignocellulosic materials affected the panels in a secondary manner; its influence was observed when the panels were evaluated after contact with water for long periods of time, such as in TS24 h and MOR and MOE after accelerated ageing.

Eucalyptus and sugarcane panels had the best results in terms of the evaluated properties and thus, could be considered for potential use as non-structural walls. However, the banana pseudostem coconut shell and coffee husk panels had the worst results and under these conditions, should not be used in building.

Author Contributions: P.F.P.F.: conceptualization, investigation, methodology, formal analysis, data curation, writing—original draft, project administration, funding acquisition. R.F.M.: methodology, formal analysis, investigation, data curation, writing—review. D.B.M.: methodology, formal analysis, data curation. J.L.P.: methodology, formal analysis, investigation, writing—review. D.C.: formal analysis, investigation, writing—review. M.B.: investigation, formal analysis, resources, writing—review and editing. All authors have read and agreed to the published version of the manuscript.

Funding: This research was funded by the Minas Gerais State Agency for Research and Development (FAPEMIG Grant n. CAG-APQ-01100-15).

Acknowledgments: The authors would like to thank the Minas Gerais State Agency for Research and Development (FAPEMIG Grant n. CAG-APQ-01100-15), the National Council of Technological and Scientific Development (CNPq), the Coordination for the Improvement of Higher Education Personnel (CAPES).

Conflicts of Interest: The authors declare that they have no known competing financial interests or personal relationships that could have appeared to influence the work reported in this paper.

References

1. Lisboa, F.J.N.; Scatolino, M.V.; de Paula Protásio, T.; Júnior, J.B.G.; Marconcini, J.M.; Mendes, L.M. Lignocellulosic Materials for Production of Cement Composites: Valorization of the Alkali Treated Soybean Pod and Eucalyptus Wood Particles to Obtain Higher Value-Added Products. *Waste Biomass Valorization* **2020**, *11*, 2235–2245. [[CrossRef](#)]
2. Karade, S.R. Cement-Bonded Composites from Lignocellulosic Wastes. *Constr. Build. Mater.* **2010**, *24*, 1323–1330. [[CrossRef](#)]
3. Barbari, M.; Monti, M.; Rossi, G.; Simonini, S.; Guerri, F.S. Simple Methods and Tools to Determine the Mechanical Strength of Adobe in Rural Areas. *J. Food Agric. Environ.* **2014**, *12*, 904–909.
4. Conti, L.; Goli, G.; Monti, M.; Pellegrini, P.; Rossi, G.; Barbari, M. Simplified Method for the Characterization of Rectangular Straw Bales (RSB) Thermal Conductivity. *IOP Conf. Ser. Mater. Sci. Eng.* **2017**, *245*. [[CrossRef](#)]
5. Cevallos, O.A.; Olivito, R.S. Effects of Fabric Parameters on the Tensile Behaviour of Sustainable Cementitious Composites. *Compos. Part B Eng.* **2015**, *69*, 256–266. [[CrossRef](#)]
6. Teixeira, J.N.; Silva, D.W.; Vilela, A.P.; Savastano Junior, H.; de Siqueira Brandão Vaz, L.E.V.; Mendes, R.F. Lignocellulosic Materials for Fiber Cement Production. *Waste Biomass Valorization* **2020**, *11*, 2193–2200. [[CrossRef](#)]
7. Eichhorn, S.J.; Baillie, C.A.; Zafeiropoulos, N.; Mwaikambo, L.Y.; Ansell, M.P.; Dufresne, A.; Entwistle, K.M.; Herrera-Franco, P.J.; Escamilla, G.C.; Groom, L.; et al. Current International Research into Cellulosic Fibres and Composites. *J. Mater. Sci.* **2001**, *36*, 2107–2131. [[CrossRef](#)]
8. Habibi, Y.; El-Zawawy, W.K.; Ibrahim, M.M.; Dufresne, A. Processing and Characterization of Reinforced Polyethylene Composites Made with Lignocellulosic Fibers from Egyptian Agro-Industrial Residues. *Compos. Sci. Technol.* **2008**, *68*, 1877–1885. [[CrossRef](#)]

9. Mendes, R.F.; Vilela, A.P.; Farrapo, C.L.; Mendes, J.F.; Tonoli, G.H.D.; Mendes, L.M. Lignocellulosic residues in cement-bonded panels. In *Sustainable and Nonconventional Construction Materials Using Inorganic Bonded Fibre Composites*, 1st ed.; Junior, H.S., Fiorelli, J., Santos, S.F., Eds.; Woodhead Publishing: Cambridge, UK, 2017; pp. 3–16.
10. Olorunnisola, A.O. Effects of Husk Particle Size and Calcium Chloride on Strength and Sorption Properties of Coconut Husk-Cement Composites. *Ind. Crops Prod.* **2009**, *29*, 495–501. [[CrossRef](#)]
11. Fan, M.; Ndikontar, M.K.; Zhou, X.; Ngamveng, J.N. Cement-Bonded Composites Made from Tropical Woods: Compatibility of Wood and Cement. *Constr. Build. Mater.* **2012**, *36*, 135–140. [[CrossRef](#)]
12. Soroushian, P.; Aouadi, F.; Chowdhury, H.; Nossoni, A.; Sarwar, G. Cement-Bonded Straw Board Subjected to Accelerated Processing. *Cem. Concr. Compos.* **2004**, *26*, 797–802. [[CrossRef](#)]
13. Cabral, M.; Zegan, D.; Palacios, J.H.; Godbout, S.; Fiorelli, J.; Savastano, H.; Gutierrez-Pacheco, S.; Lagacé, R. Potential Use of Agricultural Biomass for Cement Composite Materials: Aptitude Index Development and Validation. In Proceedings of the CSBE/SCGAB 2016 Annual Conference Halifax World Trade and Convention Centre, Halifax, NS, Canada, 3–6 July 2016. Paper No. CSBE16-056.
14. Fonseca, C.S.; Silva, M.F.; Mendes, R.F.; Hein, P.R.G.; Zangiaco, A.L.; Savastano, H.; Tonoli, G.H.D. Jute Fibers and Micro/Nanofibrils as Reinforcement in Extruded Fiber-Cement Composites. *Constr. Build. Mater.* **2019**, *211*, 517–527. [[CrossRef](#)]
15. Mármol, G.; Savastano, H.; Monzó, J.M.; Borrachero, M.V.; Soriano, L.; Payá, J. Portland Cement, Gypsum and Fly Ash Binder Systems Characterization for Lignocellulosic Fiber-Cement. *Constr. Build. Mater.* **2016**, *124*, 208–218. [[CrossRef](#)]
16. Ferraz, J.M. Production and Properties of Coir (*Cocos nucifera* L.) Fibre Panels Mixed with Portland Cement. Master's Thesis, University of Brasília, Brasília, Brazil, 2011.
17. Asgher, M.; Ahmad, Z.; Iqbal, H.M.N. Alkali and Enzymatic Delignification of Sugarcane Bagasse to Expose Cellulose Polymers for Saccharification and Bio-Ethanol Production. *Ind. Crops Prod.* **2013**, *44*, 488–495. [[CrossRef](#)]
18. Browning, B.L. *The Chemistry of Wood*; Interscience: New York, NY, USA, 1963.
19. Brazilian Association of Technical Standards. NBR 14853, *Wood—Determination of Ethane-Toluene-Soluble Material and Dichloromethane and Acetone*; Brazilian Association of Technical Standards: Rio de Janeiro, Brazil, 2010.
20. Brazilian Association of Technical Standards. NBR 7989, *Cellulosic Pulp and Wood—Determination of Acid-Insoluble Lignin*; Brazilian Association of Technical Standards: Rio de Janeiro, Brazil, 2010.
21. Brazilian Association of Technical Standards. NBR 13999, *Paper, Paperboard, Cellulosic Pulp and Wood: Determination of Th Residue (Ash) After Incineration at 525 °C*; Brazilian Association of Technical Standards: Rio de Janeiro, Brazil, 2017.
22. Brazilian Association of Technical Standards. NBR 11941, *Wood: Determination of Basic Density*; Brazilian Association of Technical Standards: Rio de Janeiro, Brazil, 2003.
23. Souza, M.R. Durability of Cement-Bonded Particle Board Made Conventionally and Carbon Dioxide Injection. Ph.D. Thesis, University of Idaho, Moscow, ID, USA, 1994.
24. American Society for Testing and Material. ASTM D1037, *Standard Methods of Evaluating the Properties of Wood-Base Fibre and Particle Panel Materials*; American Society for Testing and Material: West Conshohocken, PA, USA, 2016.
25. American Society for Testing and Material. ASTM C948, *Test Method for Dry and Wet Bulk Density, Water Absorption, and Apparent Porosity of Thin Sections of Glass-Fiber Reinforced Concrete*; American Society for Testing and Material: West Conshohocken, PA, USA, 1981.
26. Deutsches Institut Fur Normung. DIN 52362, *Testing of Wood Chipboards. Bending Test. Determination of Bending Strength*; Deutsches Institut Fur Normung: Berlin, Germany, 1982.
27. Almeida, A.E.F.S.; Tonoli, G.H.D.; Santos, S.F.; Savastano, H. Improved Durability of Vegetable Fiber Reinforced Cement Composite Subject to Accelerated Carbonation at Early Age. *Cem. Concr. Compos.* **2013**, *42*, 49–58. [[CrossRef](#)]
28. European Committee for Standardization. EN 494, *Fibre-Cement Profiled Sheets and Fittings. Product Specification and Test Methods*; European Committee for Standardization: Brussels, Belgium, 1994.
29. Demsar, J.; Leban, G.; Zupan, B. FreeViz—An intelligent visualization approach for class-labeled multidimensional data sets. In Proceedings of the Intelligent Data Analysis in Medicine and Pharmacology (IDAMAP 2005), Aberdeen, UK, 24 July 2005; Springer: Berlin/Heidelberg, Germany; pp. 61–66.

30. Demšar, J.; Leban, G.; Zupan, B. FreeViz-An Intelligent Multivariate Visualization Approach to Explorative Analysis of Biomedical Data. *J. Biomed. Inform.* **2007**, *40*, 661–671. [[CrossRef](#)]
31. QGIS Development Team. QGIS Geographic Information System—Open Source Geospatial Foundation Project. 2017. Available online: <http://www.qgis.org> (accessed on 3 June 2019).
32. Congedo, L. Semi-Automatic Classification Plugin Documentation. *Release 4.8.0.1*. 2016. Available online: https://www.researchgate.net/publication/307593091_Semi-Automatic_Classification_Plugin_Documentation_Release_6011 (accessed on 21 May 2020).
33. Onuaguluchi, O.; Banthia, N. Plant-Based Natural Fibre Reinforced Cement Composites: A Review. *Cem. Concr. Compos.* **2016**, *68*, 96–108. [[CrossRef](#)]
34. Fiorelli, J.; Gomide, C.A.; Lahr, F.A.R.; do Nascimento, M.F.; de Lucca Sartori, D.; Ballesteros, J.E.M.; Bueno, S.B.; Belini, U.L. Physico-Chemical and Anatomical Characterization of Residual Lignocellulosic Fibers. *Cellulose* **2014**, *21*, 3269–3277. [[CrossRef](#)]
35. Miller, D.; Moslemi, A. Wood-Cement Composites: Effect of Model Compounds on Hydration Characteristics and Tensile Strength. *Wood Fiber Sci.* **1991**, *23*, 472–482.
36. Fernandez, E.C.; Taja-On, V.P. The use and processing of rice straw in the manufacture of cement-bonded fibreboard. In *Wood-Cement Composites in the Asia-Pacific Region, Proceedings of the 5th Pacific Rim Bio-based Composites Symposium, Canberra, Australia, 10 December 2000*; Evans, P.D., Ed.; Australian Centre for International Agricultural Research: Canberra, ACT, Australia; pp. 49–54.
37. Campbell, A.G. Recycling and disposing of wood ash. *Tappi J.* **1990**, *73*, 141–146.
38. Anglès, M.N.; Reguant, J.; Martínez, J.M.; Farriol, X.; Montané, D.; Salvadó, J. Influence of the Ash Fraction on the Mass Balance during the Summative Analysis of High-Ash Content Lignocellulosics. *Bioresour. Technol.* **1997**, *59*, 185–193. [[CrossRef](#)]
39. Yan, L.; Chouw, N.; Jayaraman, K. Flax Fibre and Its Composites—A Review. *Compos. Part B Eng.* **2014**, *56*, 296–317. [[CrossRef](#)]
40. *Bison Wood-Cement Board*; Springer: New York, NY, USA, 2017; p. 10.
41. Nazerian, M.; Ghalehno, M.D.; Gozali, E. Effects of Wood Species, Particle Sizes and Dimensions of Residue Obtained from Trimming of Wood-Cement Composites on Physical and Mechanical Properties of Cement-Bonded Particleboard. *Wood Mater. Sci. Eng.* **2011**, *6*, 196–206. [[CrossRef](#)]
42. Rana, M.N.; Islam, M.N.; Nath, S.K.; Das, A.K.; Ashaduzzaman, M.; Shams, M.I. Properties of Low-Density Cement-Bonded Composite Panels Manufactured from Polystyrene and Jute Stick Particles. *J. Wood Sci.* **2019**, *65*, 1–10. [[CrossRef](#)]
43. Madsen, B.; Thygesen, A.; Lilholt, H. Plant Fibre Composites—Porosity and Volumetric Interaction. *Compos. Sci. Technol.* **2007**, *67*, 1584–1600. [[CrossRef](#)]
44. Laborel-Préneron, A.; Aubert, J.E.; Magniont, C.; Tribout, C.; Bertron, A. Plant Aggregates and Fibers in Earth Construction Materials: A Review. *Constr. Build. Mater.* **2016**, *111*, 719–734. [[CrossRef](#)]
45. Dhakal, H.N.; Zhang, Z.Y.; Richardson, M.O.W. Effect of Water Absorption on the Mechanical Properties of Hemp Fibre Reinforced Unsaturated Polyester Composites. *Compos. Sci. Technol.* **2007**, *67*, 1674–1683. [[CrossRef](#)]
46. Nasser, R.A.; Salem, M.Z.M.; Al-Mefarrej, H.A.; Aref, I.M. Use of Tree Pruning Wastes for Manufacturing of Wood Reinforced Cement Composites. *Cem. Concr. Compos.* **2016**, *72*, 246–256. [[CrossRef](#)]
47. Barbari, M.; Monti, M.; Rossi, G.; Simonini, S.; Guerri, F.S. Proposal for a Simple Method of Structural Calculation for Ordinary Earthen Buildings in Rural Areas. *J. Food Agric. Environ.* **2014**, *12*, 897–903.
48. Lobão, M.S.; Della Lúcia, R.M.; Moreira, M.S.S.; Gomes, A. Caracterização Das Propriedades Físico-Mecânicas Da Madeira de Eucalipto Com Diferentes Densidades. *Rev. Árvore* **2004**, *28*, 889–894. [[CrossRef](#)]
49. Rodrigues, J.; Souza, J.A.; Fujiyama, R. Polymeric composites reinforced with natural fibers from Amazon manufactured by infusion. *Rev. Matéria* **2015**, *20*, 946–960. [[CrossRef](#)]
50. Pereira, T.G.T.; Mendes, J.F.; Oliveira, J.E.; Marconcini, J.M.; Mendes, R.F. Effect of Reinforcement Percentage of Eucalyptus Fibers on Physico-Mechanical Properties of Composite Hand Lay-up with Polyester Thermosetting Matrix. *J. Nat. Fibers* **2019**, *16*, 806–816. [[CrossRef](#)]
51. Farrapo, C.L.; Fonseca, C.S.; Pereira, T.G.T.; Tonoli, G.H.D.; Junior, H.S.; Mendes, R.F. Cellulose Associated with Pet Bottle Waste in Cement Based Composites. *Mater. Res.* **2017**, *20*, 1380–1387. [[CrossRef](#)]
52. Pacheco-Torgal, F.; Jalali, S. Cementitious Building Materials Reinforced with Vegetable Fibres: A Review. *Constr. Build. Mater.* **2011**, *25*, 575–581. [[CrossRef](#)]

53. MacVicar, R.; Matuana, L.M.; Balatinecz, J.J. Aging Mechanisms in Cellulose Fiber Reinforced Cement Composites. *Cem. Concr. Compos.* **1999**, *21*, 189–196. [[CrossRef](#)]
54. Shahzad, A. Mechanical properties of lignocellulosic fibre composites. In *Lignocellulosic Fibre and Biomass-Based Composite Materials*, 1st ed.; Jawaid, M., Paridah, M.T., Saba, N., Eds.; Woodhead Publishing: Cambridge, UK, 2017; pp. 193–223.
55. Lepage, E.S. *Manual de Preservação de Madeiras*; Instituto de Pesquisas Tecnológicas de São Paulo: São Paulo, Brazil, 1986.
56. Fiorelli, J.; Curtolo, D.D.; Barrero, N.G.; Savastano, H.; Pallone, E.M.J.A.; Johnson, R. Particulate Composite Based on Coconut Fiber and Castor Oil Polyurethane Adhesive: An Eco-Efficient Product. *Ind. Crops Prod.* **2012**, *40*, 69–75. [[CrossRef](#)]

Publisher's Note: MDPI stays neutral with regard to jurisdictional claims in published maps and institutional affiliations.



© 2020 by the authors. Licensee MDPI, Basel, Switzerland. This article is an open access article distributed under the terms and conditions of the Creative Commons Attribution (CC BY) license (<http://creativecommons.org/licenses/by/4.0/>).